Monte-Carlo Methods in Financial Modeling

Chuanshu Ji, Tao Wang and Leicheng Yin

Abstract The last decade has witnessed fast growing applications of Monte-Carlo methodology to a wide range of problems in financial economics. This chapter consists of two topics: market microstructure modeling and Monte-Carlo dimension reduction in option pricing. Market microstructure concerns how different trading mechanisms affect asset price formation. It generalizes the classical asset pricing theory under perfect market conditions by incorporating various friction factors, such as asymmetric information shared by different market participants (informed traders, market makers, liquidity traders, et al.), and transaction costs reflected in bid-ask spreads. The complexity of those more realistic dynamic models presents significant challenges to empirical studies for market microstructure. In this work, we consider some extensions of the seminal sequential trade model in Glosten and Milgrom (Journal of Financial Economics, 14(1), 71–100, 1985) and perform Bayesian Markov chain Monte-Carlo (MCMC) inference based on the trade and quote (TAQ) database in Wharton Research Data Services (WRDS). As more and more security derivatives are constructed and traded in financial markets, it becomes crucial to price those derivatives, such as futures and options. There are two popular approaches for derivative pricing: the analytical approach sets the price function as the solution to a PDE with boundary conditions and solves it numerically by finite difference etc.; the probabilistic approach expresses the price of a derivative as the conditional expectation under a risk neutral measure and computes it via numerical integration. Adopting the second approach, we notice the required integration is often performed over a high dimensional state space in which state variables are financial time series. A key observation is for a broad class of stochastic volatility (SV) models, the con-

C. Ji (✉)
Department of Statistics and Operations Research, University of North Carolina, Chapel Hill, NC 27599-3260, USA
e-mail: cji@email.unc.edu

T. Wang
Bank of America Merrill Lynch,
Bank of America Tower, One Bryant Park, New York, NY 10036, USA

L. Yin
Exelon Business Services Company, Enterprise Risk Management,
Chase Tower 10 S. Dearborn St, Chicago, IL 60603, USA

D.-G. Chen and J.D. Chen (eds.), *Monte-Carlo Simulation-Based Statistical Modeling*, ICSA Book Series in Statistics, DOI 10.1007/978-981-10-3307-0_14

ditional expectations representing related option prices depend on high-dimensional volatility sample paths through only some 2D or 3D summary statistics whose samples, if generated, would enable us to avoid brute force Monte-Carlo simulation for the underlying volatility sample paths. Although the exact joint distributions of the summary statistics are usually not known, they could be approximated by distribution families such as multivariate Gaussian, gamma mixture of Gaussian, log-normal mixture of Gaussian, etc. Parameters in those families can be specified by calculating the moments and expressing them as functions of parameters in the original SV models. This method improves the computational efficiency dramatically. It is particularly useful when prices of those derivatives need to be calculated repeatedly as a part of Bayesian MCMC calibration for SV models.

1 Hierarchical Modeling in Market Microstructure Studies

The research in financial economics becomes more necessary after the financial crisis, with statistics playing an important role in such studies. Several milestones in modern finance, such as capital asset pricing model (CAPM), Black-Scholes-Merton derivatives pricing, hold under certain perfect market conditions, i.e. the market is fully efficient with no taxes, no transaction costs, no bid-ask spreads, unlimited short-selling, and all market participants sharing the same information, to name just a few. Those assumptions are clearly violated in real financial markets, evidenced by many empirical studies. Market microstructure concerns friction factors, aims to understand how asset price formation is affected by various trading mechanisms.

In this work, we will focus on two aspects of market microstructure that attract most attentions from financial economists: asymmetric information and bid/ask spreads. We will follow the model-based approach in the seminal work of Glosten and Milgrom (1985), referred to as G-M model in what follows. It is a sequential trade model assuming risk neutrality and a quote-driven protocol. The market maker posts bid and ask prices in every (discrete) time unit based on which traders place their orders. There are certain informed traders among other uninformed traders in the market, and the proportion of informed traders is represented by a parameter α. The information asymmetry induces adverse selection costs that force the market maker to quote different prices for buying and selling, leading to the bid-ask spread. The spread is a premium the market maker demands for trading with informed traders. A special feature in G-M model is to present explicitly how bid and ask prices change over time and are influenced by different trading orders.

Our research concerns empirical studies for G-M model and its extensions using real market data. Due to the complexity of many market microstructure models such as G-M, systematic model-based empirical studies are relatively lacking compared to the development of theoretical models and model-free descriptive data analysis. A noticeable contribution is Hasbrouck (2009) which considers an extension of Roll model (cf. Roll 1984) and uses the Gibbs sampler to estimate the effective trading cost and trading direction. To validate the method, a high correlation 0.965 is calculated

between the Gibbs sampler estimates of the effective cost and the descriptive estimates based on high frequency TAQ data. The sophisticated hierarchical dynamic structure in G-M model presents a challenge to model-based inference using real market data. Little has been done in this direction. Das (2005) takes a useful step by presenting an algorithm for computing approximate solutions to the bid/ask prices and runs a simulation study under a modified G-M model. It helps us learn from the market maker's perspective, and paves a road for further studies.

In this work, we consider further extensions of G-M model and perform Bayesian MCMC inference based on the TAQ database in WRDS. Both the asymmetric information and bid-ask spread issues are addressed. To the best of our knowledge, our work is the first attempt at inference on market microstructure models of G-M type based on intra-day data. Since the main focus of this chapter is implementation of MCMC algorithms, some other useful results we developed along this line are not included here, such as incorporation of GARCH (1,1) model for the volatility of asset returns which furthermore improves the model fitting. More details are available in Tao Wang's Ph.D. thesis (cf Wang 2014) upon request.

1.1 The Model

The following setting for market microstructure is assumed:

- Let V_t denote the true underlying value (logarithmic share price) of a stock at time $t = 0, 1, \ldots$ The stock dynamics follows a random walk $V_t = V_{t-1} + \epsilon_t$, where the innovations $\epsilon_1, \epsilon_2, \ldots$ are iid $N(0, \sigma^2)$ random variables with parameter $\sigma > 0$.
- A single market maker sets the ask price A_t and the bid price B_t for one share of the stock at t.
- Traders enter the market sequentially. Each of them can buy the stock at the price A_t, or sell the stock at B_t. There are two types of traders: uninformed and informed. An uninformed trader (assumed not knowing V_t) will place a buy or sell order with equal probability η, or choose not to trade with probability $1 - 2\eta$. An informed trader, who is assumed to know V_t, will place a buy order if $V_t > A_t$ or a sell order if $V_t < B_t$, or no trade order if $B_t \leq V_t \leq A_t$.
- When setting A_t and B_t at each t, the market maker, knowing neither the type of the trader nor the true value V, will face an informed trader with probability α or an uninformed one with probability $1 - \alpha$, and receive an order placed by that trader, based on which he will update his belief in such a way as defining $A_t = E_t(V \,|\, \text{Buy})$ and $B_t = E_t(V \,|\, \text{Sell})$. Here $E_t(\cdot)$ denotes the conditional expectation given the market maker's information up to t, with "Buy/Sell" inserted in the condition to reflect the most recent order type.
- Denote the observed bid/ask prices by P_t^b and P_t^a respectively and assume $P_t^b \sim N(B_t, \delta^2)$ and $P_t^a \sim N(A_t, \delta^2)$, where $\delta > 0$ measures pricing errors (small perturbation).

Following Bayes' formula we get

$$E_t[V|\text{Sell}] = \int v\ p_t(v|\text{Sell})dv$$
$$= \int v\ \frac{P_t(\text{Sell}|v)\ f_t(v)}{P_t(\text{Sell})}dv, \tag{1}$$

where $f_t(v)$ is the normal density of V_t and $P_t(\text{Sell})$, the probability of receiving a sell order at time t, is given by

$$P_t(\text{Sell}) = \alpha \int_{-\infty}^{B_t} f_t(v)dv + (1-\alpha)\eta. \tag{2}$$

Therefore,

$$B_t = \frac{1}{P_t(\text{Sell})}\int_{-\infty}^{\infty} vP_t(\text{Sell}|v)f_t(v)dv$$
$$= \frac{1}{P_t(\text{Sell})}\left(\alpha \int_{-\infty}^{B_t} vf_t(v)dv + (1-\alpha)\eta V_0\right). \tag{3}$$

Similarly, the ask price is given by

$$A_t = \frac{1}{P_t(\text{Buy})}\left(\alpha \int_{A_t}^{\infty} vf_t(v)dv + (1-\alpha)\eta V_0\right), \tag{4}$$

where $P_t(\text{Buy})$ is given by

$$P_t(\text{Buy}) = \alpha \int_{A_t}^{\infty} f_t(v)dv + (1-\alpha)\eta. \tag{5}$$

Note that determination of B_t amounts to solving (3) numerically since B_t appears on both sides of (3). Similarly, A_t is found by solving (4) numerically.

1.2 Bayesian Inference via MCMC Algorithms

The paradigm of Bayesian hierarchical modeling appears applicable for the market microstructure study in this work. The variables (called unknowns in Bayesian terms) can be classified in three layers: parameter $\theta = \{\alpha, \eta, \sigma^2, \delta^2\}$ (top layer); observed data $P^{a,b} = \{(P_t^a, P_t^b),\ t = 1, ..., T\}$ (bottom layer); unobserved latent variables $V = \{V_t,\ t = 0, 1..., T\}$ (middle layer). The presence of latent variable V hinders the traditional maximum likelihood estimation (MLE) for θ, which could be tackled by E-M algorithms (cf. Dempster et al. 1977; Meng and van Dyk 1997). We adopt

the Bayesian approach due to its flexibility of using conditional probabilities. The data $P^{a,b}$ is treated as given and the focus will be on the (joint) posterior distribution $\pi(\theta, V \mid P^{a,b})$ which is intractable analytically. Thanks to a rich class of MCMC computational algorithms, we can generate samples from a Markov chain with the state space for $\{\theta, V\}$ and the limiting distribution $\pi(\theta, V \mid P^{a,b})$. The key is to design the transition probability mechanism judiciously such that (i) the resulting chain converges to the target distribution $\pi(\theta, V \mid P^{a,b})$ rapidly (weak convergence issue); (ii) statistical parameters (as various functions of θ) can be estimated by corresponding sample statistics based on the observed MCMC sample paths accurately (variance reduction issue). There is a huge literature for MCMC. See Robert and Casella (2004), Brooks et al. (2011) for an in-depth coverage of basic MCMC theory and many related issues in applications.

In what follows, several elements in the proposed MCMC algorithm are described. See Appendix 1 for more details in implementation.

1.2.1 Priors

Assume the four components of θ are independent under the prior π. For α, a conjugate beta prior is adopted with its mode close to 0.1 because the proportion of informed traders in the market is relatively small. A uniform prior over the interval $(0, 1/2)$ for η is adopted, i.e. no information other than the restriction $0 < 2\eta < 1$ is used. For the volatility parameter σ^2, either a conjugate inverse gamma prior or uniform prior is used. For δ^2, we use a uniform prior over a small interval. Having specified the prior, the posterior distribution can be derived accordingly.

1.2.2 Metropolis-Hastings Within Gibbs

MCMC is a repertoire of algorithms among which Metropolis-Hastings algorithm (M-H) and the Gibbs sampler (GS) are the most popular ones. GS reflects a natural divide-and-conquer strategy when the state space is multi-dimensional. A one step transition of the MCMC chain amounts to cycling through a sequence of partitioning blocks of the state space, where each block can contain just a single variable or be a vector of several components. When updating one block, the states of other blocks remain fixed. M-H is an acceptance-rejection sampling scheme applied to Markov chains. It is very useful when direct sampling from a probability density becomes intractable, and it also has an advantage that we only need to know the density up to a normalizing constant factor. Although GS is shown to be a special case of M-H mathematically, most people in the MCMC community still consider them separately because they really represent very different ideas. We apply *Metropolis-Hastings within Gibbs* (MHwGS) to our setting. Using superscripts for MCMC iterations, the transition from step n to step $n + 1$ will follow

GS step: Partition the state space into k disjoint blocks and express the state variable as $x = \{x_1, ..., x_k\}$. Without loss of generality, let the updating follow a natural order $x_1 \to x_2 \to \cdots \to x_k$ in one iteration. Having done the updating $x_j^{(n)} \to x_j^{(n+1)}$ for blocks $j < i$, we are to update $x_i^{(n)}$ to $x_i^{(n+1)}$ by sampling from the conditional density $f(\cdot | \, x_j^{(n+1)}, \, j < i; \, x_j^{(n)}, \, j > i)$.

M-H step: When sampling directly from $f(\cdot | \, x_j^{(n+1)}, \, j < i; \, x_j^{(n)}, \, j > i)$ is difficult, we generate y from a proposal density $g(\cdot | \, x_j^{(n+1)}, \, j < i; \, x_j^{(n)}, \, j > i)$ first, then use the M-H ratio as a probability of accepting y and assigning $x_i^{(n+1)} = y$; otherwise stick to $x_i^{(n)}$ without a change and move forward to updating $x_{i+1}^{(n)}$, etc.

In this work, we simply let each of $\alpha, \eta, \sigma^2, \delta^2; V_1, ..., V_T$ be a block by itself (with $T + 4$ blocks in total). Choosing the proposal density g is an art. See Appendix 1 for more details.

1.2.3 Diagnostics for Convergence

Although the mathematical aspect of MCMC convergence is addressed by Marlov chain theory, an indispensable part of MCMC implementation in practice is to determine when should we stop running a chain and how should we use the samples to estimate various numerical characteristics of the target distribution. Here we only present two commonly used MCMC convergence diagnostic criteria. As many MCMC contributors commented in the literature, no single criterion can guarantee convergence and each one has its own pros and cons. A general suggestion is to use several criteria for each problem at hand.

Gelman-Rubin Method

The proposal by Gelman and Rubin (1992) consists of the following steps:

- Run $m > 1$ parallel chains of length $2n$ with over-dispersed starting values.
- Disregard the first n samples in each chain.
- Select a dynamic variable of interest, say x, and calculate its within-chain and between-chain sample variances.
- Compute the estimated variance as a weighted sum of within-chain and between-chain variances.
- Calculate the shrink factor.

The within-chain variance is given by $W = \frac{\sum_{j=1}^{m} s_j^2}{m}$, where $s_j^2 = \frac{\sum_{i=1}^{n}(x_{ij} - \bar{x}_j)^2}{n-1}$ is the sample variance for jth chain and $\bar{x}_j = \frac{\sum_{i=1}^{n} x_{ij}}{n}$. The between-chain variance is given by $B = \frac{n}{m-1} \sum_{j=1}^{m} (\bar{x}_j - \bar{\bar{x}})^2$, where $\bar{\bar{x}} = \frac{\sum_{j=1}^{m} \bar{x}_j}{m}$. B can be viewed as the variance of chain means multiplied by n. Then the estimated variance is $\widehat{Var}(x) = (1 - \frac{1}{n})W + \frac{1}{n}B$ and the shrink factor is $\hat{R} = \sqrt{\frac{\widehat{Var}(x)}{W}}$ whose value, if substantially above 1, would indicate lack of convergence. This criterion is easy to use but

appears more necessary than sufficient in the sense that it may indicate convergence prematurely if the shrink factor happens to be close to 1 by chance. A remedy is to calculate the shrink factor at several points in time (gelman.plot in R package CODA) to see whether the shrink factor is really settled or still fluctuating.

Geweke method

The procedure proposed by Geweke (1992) is based on a test for equality between means of the first and last parts of a Markov chain (by default the first 10 % and the last 50 %). If the samples are drawn from the stationary distribution of the chain, the two means are equal and Geweke statistic follows the distribution $N(0, 1)$ asymptotically.

The test statistic is a standard Z-score: the difference between the two sample means divided by its estimated standard error. The standard error is estimated from the spectral density at zero so as to take into account any autocorrelation. Hence values of Z-score that fall in the extreme tails of $N(0, 1)$ suggest that the chain has not fully converged.

If Geweke's diagnostic indicates that the first and last parts sampled from a Markov chain are not drawn from the same distribution, it may be useful to discard the first few iterations to see if the rest of the chain has "converged". The geweke.plot in R package CODA shows what happens to Geweke's Z-score when successively larger numbers of iterations are discarded from the beginning of the chain. To preserve the asymptotic conditions required for Geweke's diagnostic, the plot never discards more than half the chain.

The first half of the Markov chain is divided into several segments, then Geweke's Z-score is repeatedly calculated. The first Z-score is calculated with all iterations in the chain, the second after discarding the first segment, the third after discarding the first two segments, etc. The last Z-score is calculated using only the samples in the second half of the chain.

1.3 Simulation Study

In order to test whether our MCMC algorithms work well, we do simulation study first. In the simulation study, we specify $\alpha = 0.1$, $\eta = 0.25$, $\sigma^2 = 0.25$, $\delta^2 = 0.09$. Based on the market model in Sect. 1.1, we calculated the bid and ask prices, and then use these synthetic data to estimate the four parameters in the model by our MCMC algorithms. We run two MCMC chains, each containing 50,000 samples, and discard 10,000 burn in samples. After the burn in stage, we retain one in every 20 samples as a new path. Table 1 examines the effectiveness of the estimation strategy, showing the true value, posterior summary statistics of those parameters. We could use the posterior mean or posterior median as an estimation of the parameter.

Table 1 Summary statistics of the posterior samples for all four parameters in simulation study

Parameter	True value	Min	Median	Mean	Max	Standard error
α	0.10	0.003	0.15	0.15	0.51	0.001
η	0.25	0.00	0.23	0.25	0.50	0.002
σ^2	0.25	0.05	0.21	0.25	1.67	0.002
δ^2	0.09	0.07	0.10	0.10	0.43	0.001

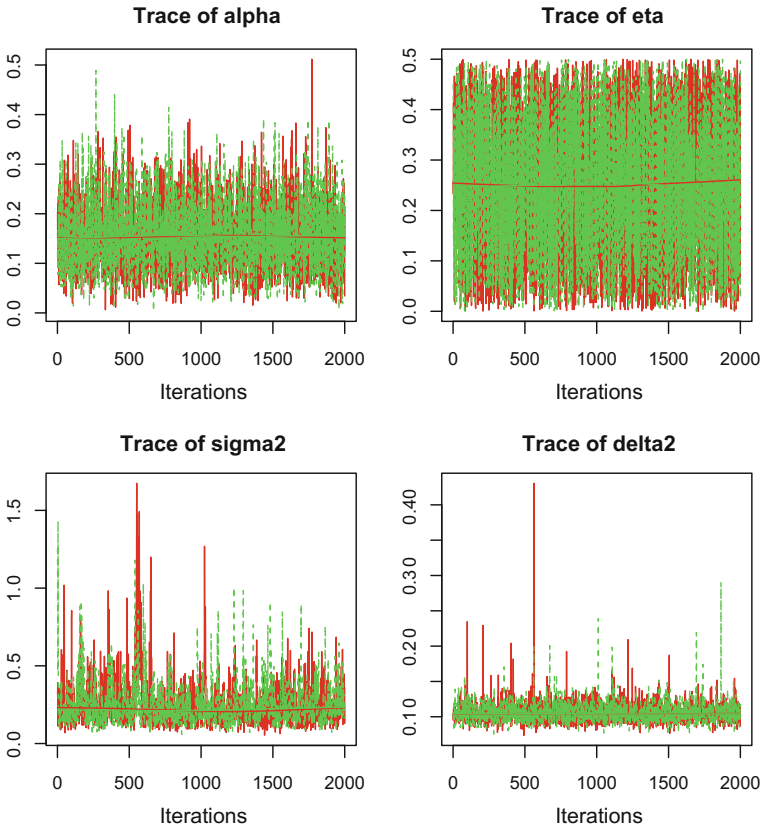

Fig. 1 Trace plot of the posterior samples in simulation study, *green* is chain 1 and *red* is chain 2

Figures 1, 2, 3 and 4 show the related convergence results of the MCMC algorithm.

Trace plots give us a direct insight of what values the posterior samples take at each iteration.

The autocorrelation plots show us how the autocorrelation changes with the increase of lag. From the autocorrelation plot, we can see except for σ^2, the autocor-

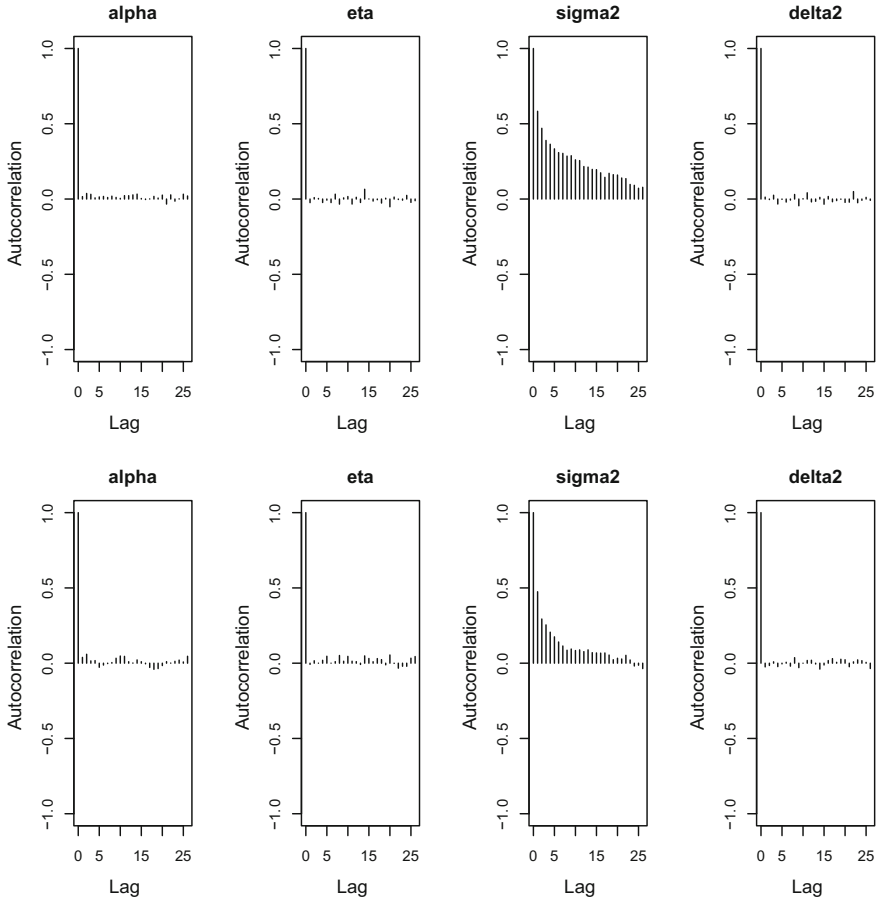

Fig. 2 Autocorrelation of the posterior samples in simulation study

relations for the other 3 parameters are near 0 at any lag. For σ^2, the autocorrelation decreases to 0 as the lag increases.

From Gelman-Rubin plot, we can see that the shrink factors for all four parameters converge to 1 after some iterations. Also, from Geweke plot, most of the Z-scores for all parameters are between -1.96 and 1.96. Both the Gelman-Rubin and Geweke plots show good MCMC convergence results.

The similarities between the posterior estimates and true values of the parameters and other convergence results indicate that our MCMC algorithm works well. Next step is to conduct empirical studies using real high frequency data.

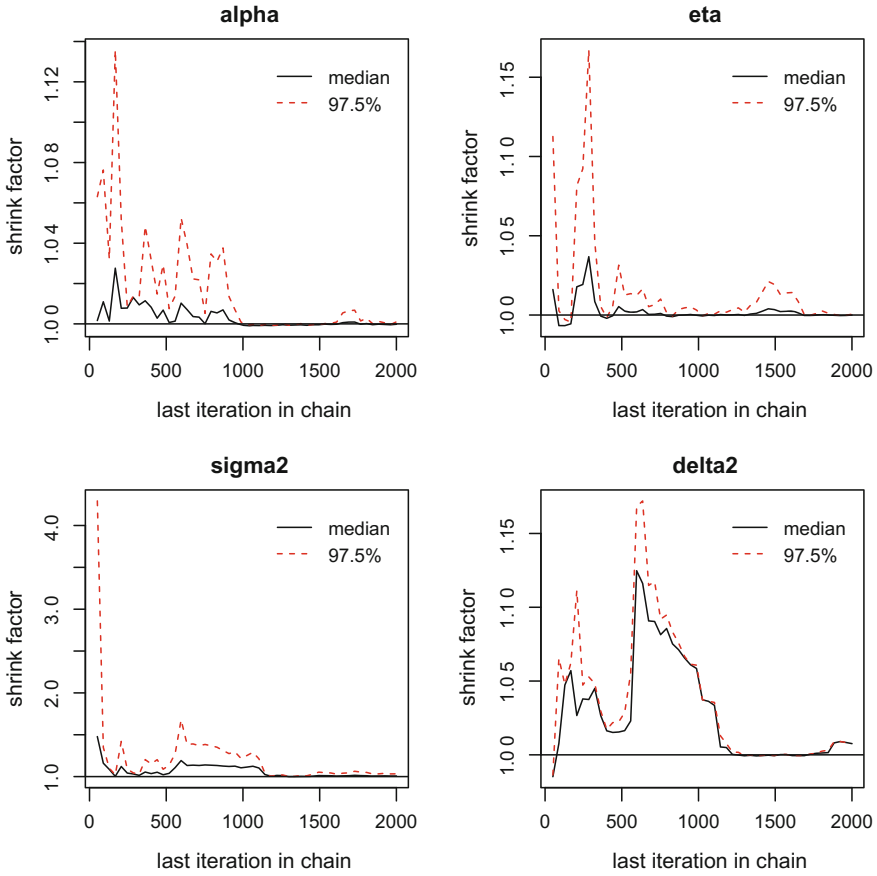

Fig. 3 Gelman-Rubin plots in simulation study. Convergence is suggested when the medians and the 97.5 percentiles approach 1

1.4 Empirical Study

1.4.1 Data

The data we used are the bid and ask prices of Microsoft stock in April, 2013 from TAQ database. TAQ contains intraday transactions data for all securities listed on the New York Stock Exchange (NYSE) and American Stock Exchange (AMEX), as well as Nasdaq National Market System (NMS) and SmallCap issues.

The data set has around 28,000,000 observations in total: over 900,000 observations on each trading day, and about 13 tradings at each time spot. There are a couple of major problems if we use raw bid and ask prices. One is computational budget constraint. The heavy computational burden would limit the sample to a relatively

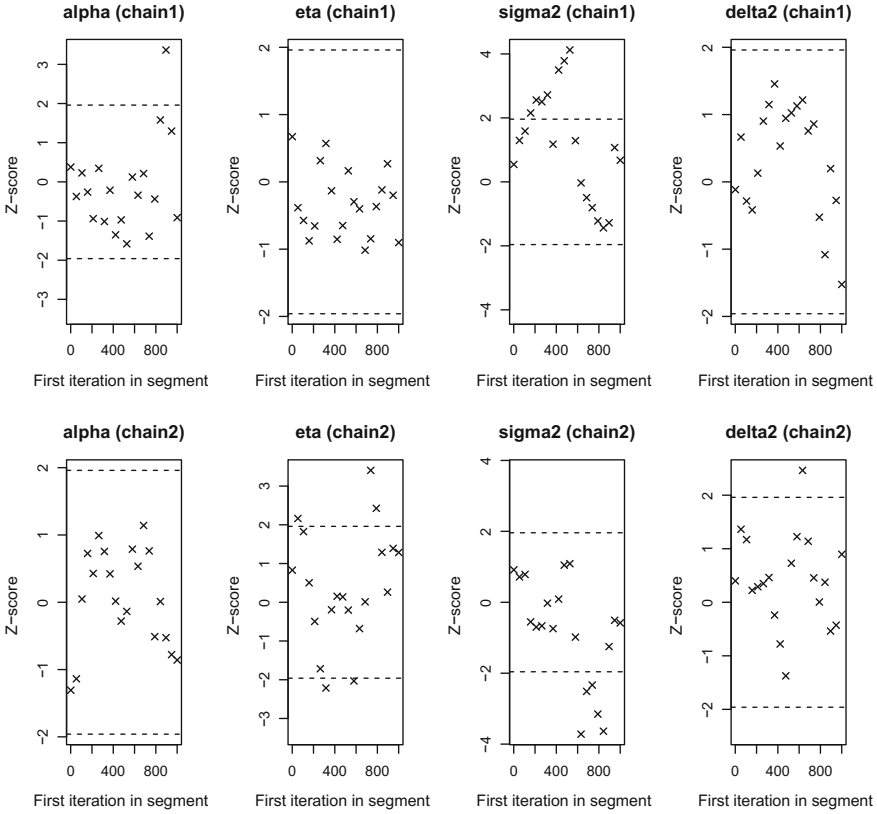

Fig. 4 Geweke plot in simulation study. Convergence is suggested when most of the Z-scores are between −1.96 and 1.96

short time horizon. Another issue is: too much noise in the original high frequency data would cause microstructure bias in inference. Therefore, our empirical study begins with some data processing:

- Missing data are deleted.
- The mean of all observations at the same trading time spot is used.
- since tradings are heavier at the beginning and the end of a trading day, while lighter around lunch time, we partition each day into 5 periods: 9:30 to 10:00, 10:00 to 11:30, 11:30 to 2:30, 2:30 to 3:30, 3:30 to 4:00 and use averages of bid/ask prices during each period.

Figure 5 shows the bid and ask prices for the cleaned data. From Fig. 1, it is hard to see the difference between the bid and ask prices since they only differ by 1 or 2 cents. Figure 6 shows a zoom-in version of Fig. 5, that plots only the first 10 bid and ask prices to help the visual effect.

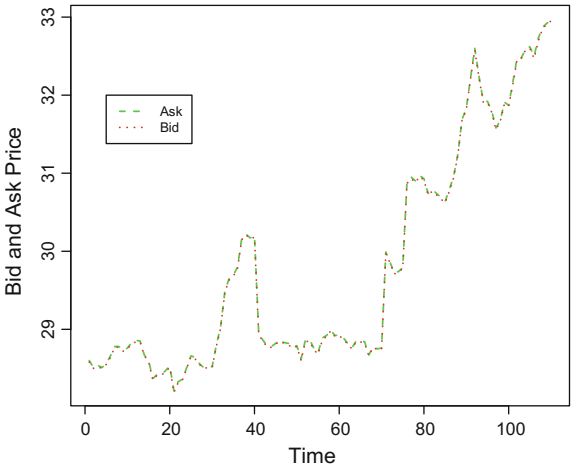

Fig. 5 Bid and ask prices for 22 consecutive trading days, x-axis represents the trading time after aggregation (5 trades per day after the aggregation of data)

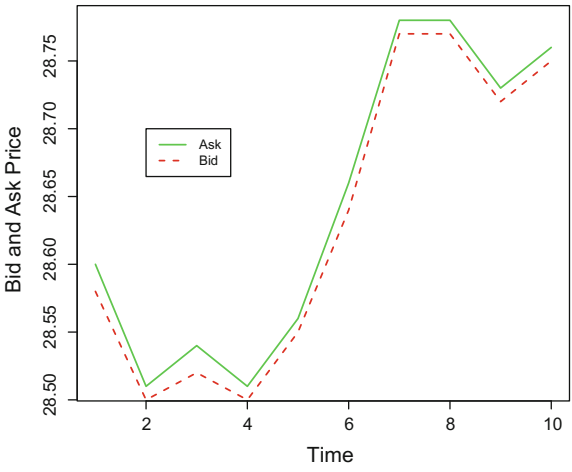

Fig. 6 Bid and ask prices for the first 2 consecutive trading days, x-axis represents the trading time after aggregation (5 trades per day after the aggregation of data)

1.4.2 Summary Statistics and MCMC Convergence

Table 2 shows the summary statistics of the posterior samples for the four parameters. Again, we could use posterior mean or posterior median as a point estimate for each parameter.

Figures 7, 8, 9 and 10 show the convergence results of the MCMC algorithm, similar to the analysis in the Simulation Study.

Table 2 Summary statistics of the posterior samples in empirical study

Parameter	Min	Median	Mean	Max	Standard error
α	0.0015	0.0856	0.0997	0.4415	0.0008
η	0.00004	0.2449	0.2477	0.5007000	0.0018
σ^2	0.0588	0.2141	0.2510	2.275	0.0019
δ^2	0.00006	0.2502	0.2509	0.4999	0.0018

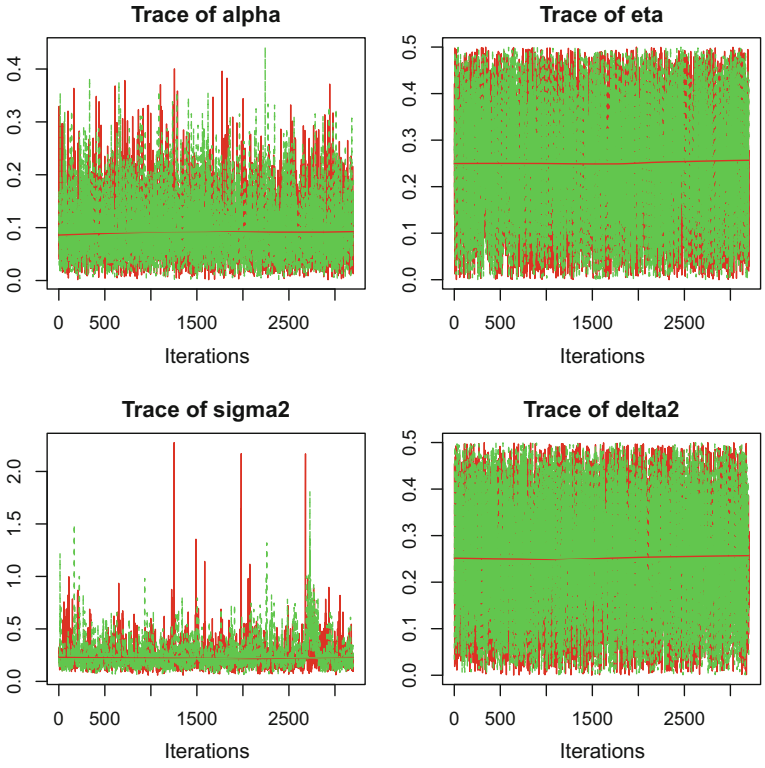

Fig. 7 Trace plot of the posterior samples in empirical study

1.5 Economic Interpretation

There are at least three sources for bid-ask spread: the adverse selection costs arising with asymmetric information, the inventory costs, and the order processing cost, which is associated with handling transactions. G-M model focuses on the first one. The extended G-M model we studied in this work also helps addressing the related issues. Besides the numerical evidence shown in Fig. 11, we also proved theoretically that the average bid-ask spread is an increasing function of α (see Wang 2014), i.e.

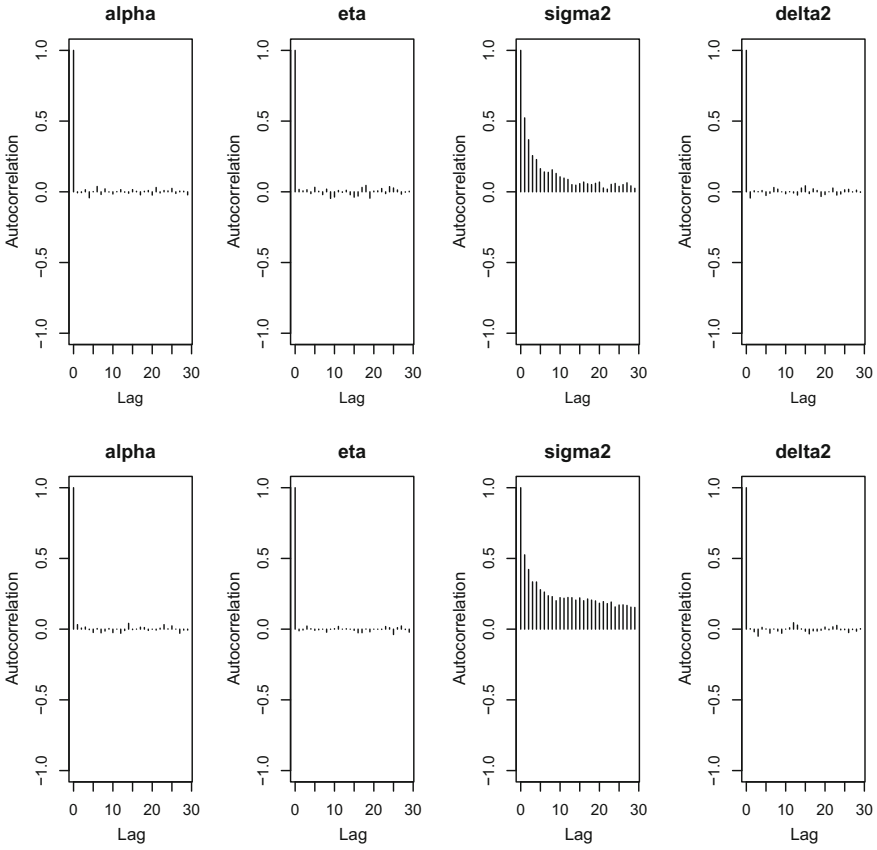

Fig. 8 Autocorrelation of the posterior samples in empirical study

the spread can be considered a premium that market makers demand for trading with agents with superior information. Another result developed in Wang (2014) is that under the extended G-M model, the bid-ask spread tends to zero at a certain rate as the number of trades go to infinity. However, this has not been shown in our empirical study, due to the limited time horizon used in the data. In addition, the bid-ask spread reflects the market maker's belief about asymmetric information. The degree of informed trading among market participants may not change in the short time period, at least from the market maker's viewpoint. This implies that the market maker makes no inference when he sees the total order imbalance at tick level. He may shift the whole bid-ask band rather than change the spread itself. Figure 12 shows the bid-ask spread for the cleaned data based on which we do not see much change of the spread over a short time period. More careful and thorough post-modeling analysis is still our ongoing project in which both in-sample (e.g. residual analysis) and out-of-sample (cross-validation) diagnostics are conducted.

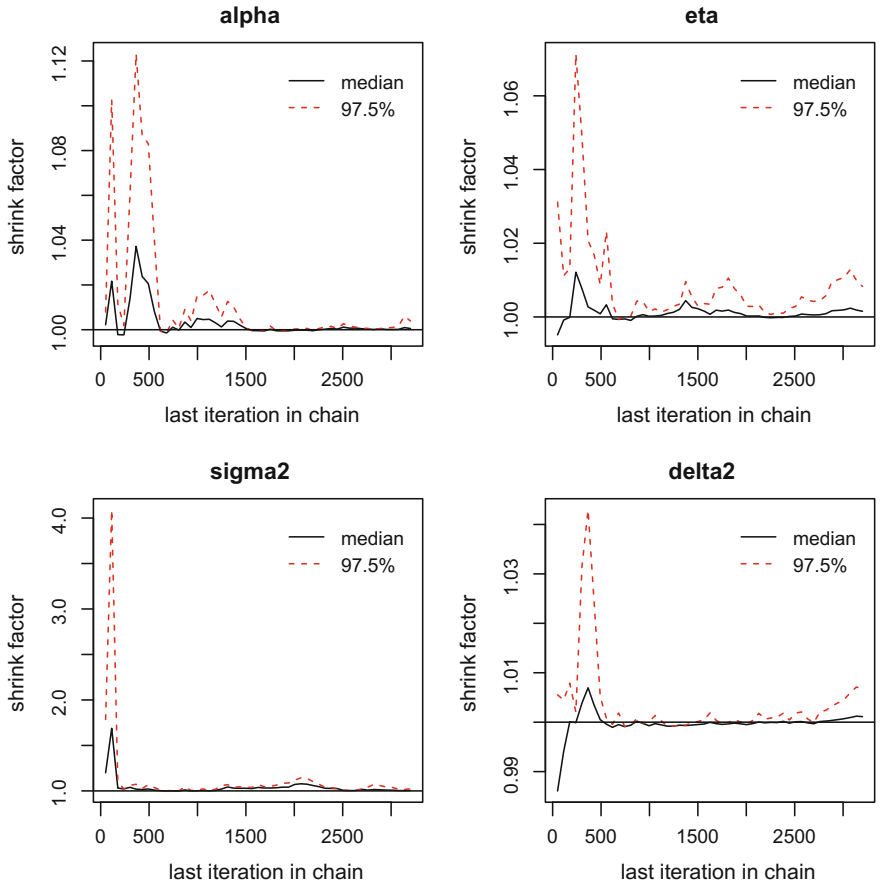

Fig. 9 Gelman-Rubin plots in empirical study. Convergence is suggested when the medians and the 97.5 percentiles approach 1

The extended G-M has conceivably made a number of unrealistic assumptions, such as the constant α for the proportion (or the impact) of informed traders in the market, and the constant trading volume associated with each trade. Modifications of those assumptions require more hard work in both theoretical and empirical studies.

1.6 Appendix 1

We provide more details of the MCMC algorithm here.

The hyperparameters in the prior distributions are set as follows:
in the beta prior for α: $\alpha_\alpha = 2,\ \beta_\alpha = 10$;

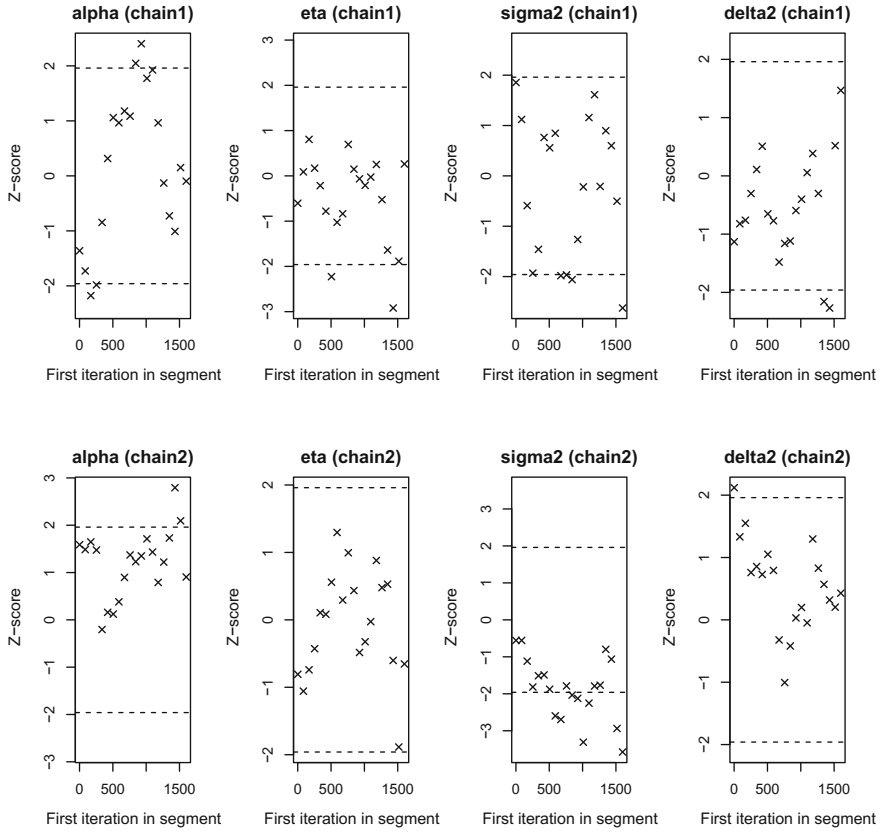

Fig. 10 Geweke plot in empirical study. Convergence is suggested when most of the Z-scores are between −1.96 and 1.96

in the inverse gamma prior for σ^2: $\alpha_\sigma = 3,\ \beta_\sigma = 1$;
in the uniform prior for σ^2: $u_{1\sigma} = 0,\ u_{2\sigma} = 0.5$;
in the uniform prior for δ^2: $u_{1\delta} = 0,\ u_{2\delta} = 0.5$.

Note that subscripts $t = 1, ..., T$ stand for real time in the model and superscripts $n = 1, ..., N$ represent the MCMC computational time.
Initialize $\alpha^{(0)}, \eta^{(0)}, \sigma^{2(0)}, \delta^{2(0)}, V_1^{(0)}, \ldots, V_T^{(0)}$, which can be assigned or sampled from the prior. A complete transition from the $(n-1)$th generation to the nth generation consists of the following steps:

Step 1: Update the latent variable $V_t^{(n)}$
For $t = 2, 3, \ldots, T-1$,

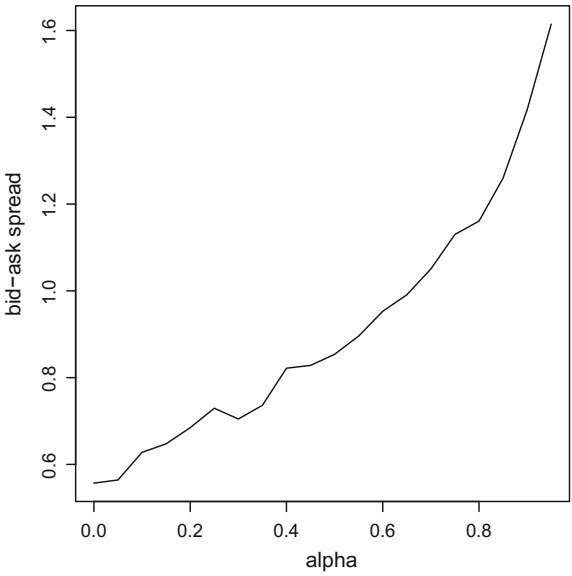

Fig. 11 The mean bid-ask spread versus α in the simulation study, the y-axis is the mean of bid-ask spreads across time using different α values

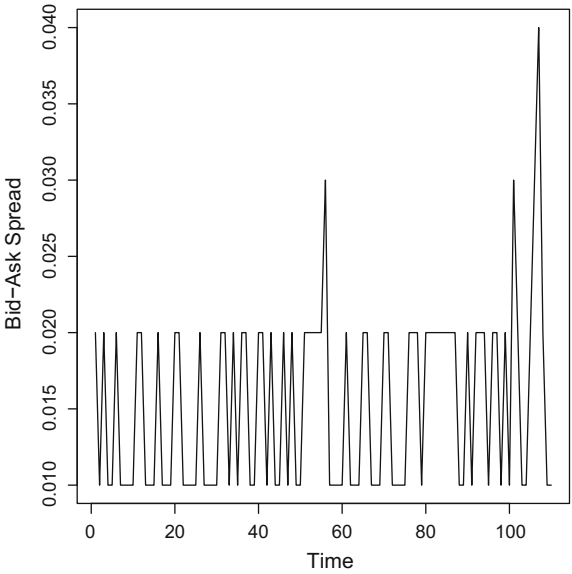

Fig. 12 The bid-ask spread versus time for the cleaned real data, the bid-ask spread does not change very much

$$
\begin{aligned}
& f(V_t^{(n)}|V^{(n-1)}, V_1^{(n)}, \ldots, V_{t-1}^{(n)}, \theta^{(n-1)}, P^a, P^b) \\
\propto\ & f(V_t^{(n)}|V_{t-1}^{(n)}, \theta^{(n-1)})\ f(V_{t+1}^{(n-1)}|V_t^{(n)}, \theta^{(n-1)}) \\
\propto\ & \exp\left[-\tfrac{(V_t^{(n)}-V_{t-1}^{(n)})^2}{2\sigma^{2(n-1)}} - \tfrac{(V_{t+1}^{(n-1)}-V_t^{(n)})^2}{2\sigma^{2(n-1)}}\right] \\
\propto\ & \exp\left\{-\tfrac{[V_t^{(n)}-\frac{V_{t-1}^{(n)}+V_{t+1}^{(n-1)}}{2}]^2}{2(\sigma^{(n-1)}/\sqrt{2})^2}\right\} \\
\sim\ & N\left(\tfrac{V_{t-1}^{(n)}+V_{t+1}^{(n-1)}}{2}, \tfrac{\sigma^{2(n-1)}}{2}\right)
\end{aligned}
$$

where $V^{(n)} = (V_1^{(n)}, \ldots, V_T^{(n)})$, and $\theta^{(n)} = (\alpha^{(n)}, \eta^{(n)}, \sigma^{2(n)}, \delta^{2(n)})$. Given all the other variables, we just sample from a normal distribution with mean $\frac{V_{t-1}^{(n)}+V_{t+1}^{(n-1)}}{2}$ and variance $\frac{\sigma^{2(n-1)}}{2}$ to get $V_t^{(n)}$.
For $t = 1$, generate $V_1^{(n)} \sim N(V_2^{(n-1)}, \sigma^{2(n-1)})$.
For $t = T$, generate $V_T^{(n)} \sim N(V_{T-1}^{(n)}, \sigma^{2(n-1)})$.

Step 2: Update $\sigma^{2(n)}$
If the prior is IG(α_σ, β_σ) (inverse gamma), then

$$
\begin{aligned}
& f(\sigma^{2(n)}|V^{(n)}, \alpha^{(n-1)}, \eta^{(n-1)}, \delta^{2(n-1)}, P^a, P^b) \\
\propto & \prod_{t=2}^{T} f(V_t^{(n)}|V_{t-1}^{(n)}, \alpha^{(n-1)}, \eta^{(n-1)}, \delta^{2(n-1)}, P^a, P^b)\ f(\sigma^{2(n)}) \\
\propto & \prod_{t=2}^{T} (\sigma^{2(n)})^{-\frac{1}{2}}\ \exp\left[-\frac{(V_t^{(n)} - V_{t-1}^{(n)})^2}{2\sigma^{2(n)}}\right]\ (\sigma^{2(n)})^{-\alpha_\sigma - 1}\ e^{-\frac{\beta_\sigma}{\sigma^{2(n)}}} \\
\propto & (\sigma^{2(n)})^{-(\frac{T-1}{2}+\alpha_\sigma)-1}\ \exp\left[-\frac{\frac{\sum_{t=2}^{T}(V_t^{(n)}-V_{t-1}^{(n)})^2}{2} + \beta_\sigma}{\sigma^{2(n)}}\right] \\
\sim & \text{IG}\left(\frac{T-1}{2} + \alpha_\sigma, \frac{\sum_{t=2}^{T}(V_t^{(n)} - V_{t-1}^{(n)})^2}{2} + \beta_\sigma\right).
\end{aligned}
$$

If the prior is Unif($u_{1\sigma}$, $u_{2\sigma}$), then

$$
\begin{aligned}
& f(\sigma^{2(n)}|V^{(n)}, \alpha^{(n-1)}, \eta^{(n-1)}, \delta^{2(n-1)}, P^a, P^b) \\
\propto & \prod_{t=2}^{T} f(V_t^{(n)}|V_{t-1}^{(n)}, \alpha^{(n-1)}, \eta^{(n-1)}, \delta^{2(n-1)}, P^a, P^b) f(\sigma^{2(n)}) \\
\propto & (\sigma^{2(n)})^{-\frac{T-1}{2}}\ \exp\left[-\frac{\sum_{t=2}^{T}(V_t^{(n)} - V_{t-1}^{(n)})^2}{2\sigma^{2(n)}}\right] I_{\{\sigma^{2(n)} \in (u_{1\sigma}, u_{2\sigma})\}}.
\end{aligned}
$$

The posterior distribution is not in a closed form, hence we need MHwGS. The procedure is as follows:

- Simulate a sample y_σ from a proposal density q_σ, which is chosen to be the prior Unif$(u_{1\sigma}, u_{2\sigma})$ here.
- Denote the posterior distribution of σ^2 by f_σ, compute the acceptance probability (M-H ratio) $\rho_\sigma = min(1, \frac{f_\sigma(y_\sigma)q_\sigma(\sigma^{(n-1)})}{f_\sigma(\sigma^{(n-1)})q_\sigma(y_\sigma)})$.
- Let $\sigma^{2(n)} = \begin{cases} y_\sigma & \text{with probability } \rho_\sigma \\ \sigma^{2(n-1)} & \text{with probability } 1-\rho_\sigma \end{cases}$.

Step 3: Update $\alpha^{(n)}$

$$f(\alpha^{(n)}|V^{(n)}, \sigma^{2(n)}, \eta^{(n-1)}, \delta^{2(n-1)}, P^a, P^b)$$
$$\propto \prod_{t=1}^{T} \exp\left[-\frac{(P_t^a - A_t)^2}{2\delta^{2(n-1)}} - \frac{(P_t^b - B_t)^2}{2\delta^{2(n-1)}}\right] (\alpha^{(n)})^{\alpha_\alpha - 1}(1-\alpha^{(n)})^{\beta_\alpha - 1}$$

where B_t, A_t is given by (3) and (4) with η, α replaced by $\eta^{(n-1)}$ and $\alpha^{(n)}$ respectively. Again, we need MHwGS:

- Simulate a sample y_α from a proposal density q_α, which is chosen to be the prior Beta$(\alpha_\alpha, \beta_\alpha)$.
- Denote the posterior of α by f_α, compute the acceptance probability $\rho_\alpha = min(1, \frac{f_\alpha(y_\alpha)q_\alpha(\alpha^{(n-1)})}{f_\alpha(\alpha^{(n-1)})q_\alpha(y_\alpha)})$.
- Let $\alpha^{(n)} = \begin{cases} y_\alpha & \text{with probability } \rho_\alpha \\ \alpha^{(n-1)} & \text{with probability } 1-\rho_\alpha \end{cases}$.

Step 4: Update $\eta^{(n)}$

$$f(\eta^{(n)}|V^{(n)}, \sigma^{2(n)}, \alpha^{(n)}, \delta^{2(n-1)}, P^a, P^b)$$
$$\propto \prod_{t=1}^{T} \exp\left[-\frac{(P_t^a - A_t)^2}{2\delta^{2(n-1)}} - \frac{(P_t^b - B_t)^2}{2\delta^{2(n-1)}}\right] I_{\{\eta^{(n)} \in (0,1/2)\}}$$

where B_t, A_t is given by (3) and (4) with η, α replaced by $\eta^{(n)}$ and $\alpha^{(n)}$ respectively. Similarly, MHwGS is applied here:

- Simulate a sample y_η from a proposal density q_η, which is chosen to be the prior distribution Unif$(0, 1/2)$.
- Denote the posterior distribution of η by f_η, compute the acceptance probability $\rho_\eta = min(1, \frac{f_\eta(y_\eta)q_\eta(\eta^{(n-1)})}{f_\eta(\eta^{(n-1)})q_\eta(y_\eta)})$.
- $\eta^{(n)} = \begin{cases} y_\eta & \text{with probability } \rho_\eta \\ \eta^{(n-1)} & \text{with probability } 1-\rho_\eta \end{cases}$.

Step 5: Update $\delta^{2(n)}$

$$f(\delta^{2(n)}|V^{(n)}, \sigma^{2(n)}, \alpha^{(n)}, \eta^{(n)}, P^a, P^b)$$
$$\propto (\delta^{2(n)})^{-T} \exp\left[-\sum_{t=1}^{T} \frac{(P_t^a - A_t)^2 + (P_t^b - B_t)^2}{2\delta^{2(n)}}\right] I_{\{\delta^{2(n)} \in (u_{1\delta}, u_{2\delta})\}}.$$

Here the needed MHwGS is given by

- Simulate a sample y_δ from a proposal density q_δ, which is chosen to be the prior Unif$(u_{1\delta}, u_{2\delta})$.
- Denote the posterior density of δ as f_δ, compute the acceptance probability $\rho_\delta = min(1, \frac{f_\delta(y_\delta)q_\delta(\delta^{2(n-1)})}{f_\delta(\delta^{2(n-1)})q_\delta(y_\delta)})$.
- Let $\delta^{2(n)} = \begin{cases} y_\delta & \text{with probability } \rho_\delta \\ \delta^{2(n-1)} & \text{with probability } 1-\rho_\delta \end{cases}$.

Step 6: Now go to Step 1 for the updating in the next iteration of transition.

2 Monte-Carlo Strategies in Option Pricing for SABR Model

In finance, an option is a contract which gives the buyer the right, but not the obligation, to buy or sell an underlying asset or instrument at a specified strike price on or before a specified date, depending on the form of the option. Because valuation of option contracts depends on a number of other variables besides the underlying asset, it is a complex task and becomes a central topic in mathematical finance. For valuation of options, cases with closed-form pricing formulas are rare with exceptions of Black-Scholes-Merton model, Hestons model, just name a few. In general, numerical computation and approximation techniques are almost always required. There are basically two approaches. The analytical approach sets the price function as the solution to a PDE with boundary conditions, which are often solved by numerical methods such as finite difference etc. The probabilistic approach expresses an option price as the conditional expectation under a risk neutral measure which needs to be computed using numerical integration. Such integration is often performed over a high dimensional state space in which state variables are time series of underlying assets or volatilities. In this situation, Monte-Carlo simulation appears inevitable.

SABR (abbreviation for **stochastic** $\alpha\beta\rho$) model enjoys the popularity in the study of stochastic volatility with applications in asset pricing and risk management. Major references include Antonov and Spector (2012), Hagan et al. (2002) and (2005), Paulot et al. (2009), Rebonado et al. (2011), among others. The main feature of the SABR model, compared to some previous models, is its capability in reproducing the dynamic behavior of volatility smiles and skews, and thus in yielding more stable results for pricing and hedging. SABR assumes that the volatility of the asset

(e.g. stock or forward) follows a geometric Brownian motion, and is correlated to the underlying forward price (leverage effect). So far almost all cited works for SABR have adopted the analytical approach using singular perturbation of the pricing function. In contrast, we take the probabilistic approach for pricing options under SABR.

The basic idea of our approach is Monte-Carlo dimension reduction using certain probability approximation schemes. Note that brute force Monte-Carlo for option pricing begins with Euler approximation that discretizes sample paths of the asset and volatility, followed by calculating the option payoff along each path then taking averages. In doing so, small steps in the discretization are needed to reduce the bias, but that would require a far greater number of simulated sample paths to reduce the variance. To alleviate the computational intensity, we observe that many pricing functionals of interest only depend on the volatility sample paths through two or three summary statistics. Therefore, it would suffice to know the joint distribution of those 2D or 3D summary statistics when calculating the option price. Our strategy will naturally be finding good approximations for the joint distribution when the exact form is not available.

After introducing SABR model and the option pricing formula, the probability approximation scheme boils down to expressing moments of some key summary statistics as functions of original model parameters. We have done this by exact analytical calculation, and obtained good results for all different ranges of parameter β, because three cases $\beta = 1$ (generalized Black-Scholes model), $\beta = 0$ (Gaussian model) and $0 < \beta < 1$ give rise to different pricing formulas. Since the basic idea is the same, we will only present the case $\beta = 1$ in this chapter and refer to the Ph.D. thesis Yin (2016) for the other two cases and the technical details.

2.1 SABR Model and Option Pricing for the Case $\beta = 1$

The risk-neutral dynamics of general SABR model is given by SDEs

$$dF(t) = r\ F(t)^{\beta} dt + \sigma(t) F(t)^{\beta} dW_1(t), \tag{6}$$

$$d\sigma(t) = \alpha\ \sigma(t) dW_2(t), \tag{7}$$

with the underlying asset value $F(t)$ (e.g. LIBOR forward rate, or forward swap rate, or stock price) and the volatility $\sigma(t)$, where r is the risk-free interest rate, $W_1(t)$ and $W_2(t)$ are two correlated standard Brownian motions with correlation coefficient ρ, i.e.

$$dW_1(t)\ dW_2(t) = \rho\ dt. \tag{8}$$

As we mentioned, the three model parameters $\alpha > 0$, $0 \leq \beta \leq 1$ and $-1 \leq \rho \leq 1$ give the reason for using the abbreviation SABR — stochastic $\alpha\beta\rho$ model, and by changing their values, a variety of interesting market behaviors can be mimicked.

The value of a European call option is defined by the expected value of discounted option payoff at maturity t_{ex}, i.e.

$$C(F_0, K) = e^{-rt_{ex}} E\left\{E_\sigma\left\{\max(F(t_{ex}) - K, 0)\right\}\right\}, \tag{9}$$

where $F_0 = F(0)$ is the present asset value, K is the strike price and $E_\sigma(\cdot)$ denotes the conditional expectation given the path $\sigma(t),\ 0 \le t \le t_{ex}$.

Consider the case $\beta = 1$ [called the *generalized BLack-Scholes* (*B-S*) *model* in th literature] and rewrite (6), (7), (8) as an equivalent form

$$dF(t) = rF(t)dt + \sigma(t)F(t)[\sqrt{1-\rho^2}dB_1(t) + \rho dB_2(t)] \tag{10}$$

$$d\sigma(t) = \alpha\sigma(t)dB_2(t) \tag{11}$$

where $B_1(t)$ and $B_2(t)$ are two independent standard Brownian motions and all other notations remain the same as defined before. We will use this form of SABR model in what follows.

Define

$$\Sigma^2 = \int_0^{t_{ex}} \sigma(u)^2 du, \tag{12}$$

$$X_1 = \int_0^{t_{ex}} \sigma(u) dB_1(u), \tag{13}$$

$$X_2 = \int_0^{t_{ex}} \sigma(u) dB_2(u). \tag{14}$$

Conditioning on the volatility path $\sigma(t),\ 0 \le t \le t_{ex}$, we have

$$\begin{aligned} &E_\sigma\left\{\max\left(F(t_{ex}) - K, 0\right)\right\} = \\ &F_0\ \exp\{rt_{ex} + \rho X_2 + \tfrac{1}{2}(1 - \rho - \sqrt{1-\rho^2} - \rho^2)\Sigma^2\}\Phi(d_1) \\ &\qquad -K\ \Phi(d_2), \end{aligned} \tag{15}$$

where Φ is the cdf of $N(0, 1)$, and d_1 and d_2 are given by

$$d_1 = d_2 + \sqrt{1-\rho^2}\ \Sigma, \tag{16}$$

$$d_2 = \frac{ln(\frac{F_0}{K}) - \frac{1}{2}(\rho + \sqrt{1-\rho^2})\ \Sigma^2 + \rho X_2 + rt_{ex}}{\sqrt{1-\rho^2}\Sigma}. \tag{17}$$

Therefore, it suffices to compute the option price $C(F_0, K)$ in (9) as the expected value under the joint distribution of (Σ^2, X_2) without simulating the entire volatility path on $[0, t_{ex}]$.

2.2 *Approximating the Distribution of* (Σ^2, X_2)

There are a couple of factors taken into account when choosing an approximate distribution for (Σ^2, X_2). Firstly, Σ^2 is positive and often has a skewed density. Secondly, X_2 is a martingale with respect to the time t_{ex}, and conditioning on $(\sigma(t), 0 \le t \le t_{ex})$, $X_2 \sim N(0, \Sigma^2)$. Hence we propose a gamma mixture of normals for the distribution of (Σ^2, X_2). Having decided the distribution family, we relate the two parameters of gamma density for Σ^2 to the first and second moments of (Σ^2, X_2), which in turn can be calculated analytically as closed forms of the original model parameters. That leads to specification of the parameters in gamma family as functions of parameters in SABR model. Similar results in using an inverse gamma mixture of normals and log-normal mixture of normals are given in Yin (2016).

Moments as functions of SABR model parameters

Denote $\sigma(0) = \sigma_0$, we have

$$
\begin{aligned}
E\{\Sigma^2\} &= \frac{\sigma_0^2}{\alpha^2}(e^{\alpha^2 t_{ex}} - 1), \\
E\{(\Sigma^2)^2\} &= \frac{2\sigma_0^4}{5\alpha^4}(\frac{1}{6}e^{6\alpha^2 t_{ex}} - e^{\alpha^2 t_{ex}} + \frac{5}{6}), \\
E\{(\Sigma^2)^3\} &= \frac{\sigma_0^6}{315\alpha^6}(e^{15\alpha^2 t_{ex}} - 7e^{6\alpha^2 t_{ex}} + 27e^{\alpha^2 t_{ex}} - 21).
\end{aligned}
$$

for every $n = 1, 2, ...,$

$$
E\{X_2^n\} = \frac{\sigma_0^n}{\alpha^n}\sum_{k=0}^{n}(-1)^{n-k}\binom{n}{k}e^{\frac{1}{2}k(k-1)\alpha^2 T}.
$$

in particular,

$$
\begin{aligned}
E\{X_2\} &= 0, \\
E\{X_2^2\} &= \frac{\sigma_0^2}{\alpha^2}(e^{\alpha^2 t_{ex}} - 1).
\end{aligned}
$$

moreover,

$$
Cov(\Sigma^2, X_2) = \frac{\sigma_0^3}{3\alpha^3}(e^{3\alpha^2 t_{ex}} - 3e^{\alpha^2 t_{ex}} + 2).
$$

Connections between parameters in the gamma mixture of normals and moments of (Σ^2, X_2)

For convenience, denote the needed moments by

$$
\begin{aligned}
E(X_2^2) = E(\Sigma^2) &\triangleq S, \\
E[(\Sigma^2)^2] &\triangleq \Delta, \\
Cov(\Sigma^2, X_2) &\triangleq \Gamma,
\end{aligned}
$$

where the first equality is due to Ito's isometry, and $S\Delta \geq \Gamma^2$ follows from Cauchy-Schwarz inequality.

Now we have

Proposition 14.1 *Let* $\Sigma^2 \sim Gamma(\kappa, \theta)$ *and* $X_2 \sim N(a_0 + a_1\Sigma^2, b\Sigma^2)$ *conditioning on the path* $\{\sigma(t), 0 \leq t \leq t_{ex}\}$ *where the constants* $a_0 \in I\!R$, $a_1 \in I\!R$, $b > 0$ *and the parameters* κ, θ *are given by*

$$
\begin{aligned}
\kappa &= \frac{S^2}{\Delta - S^2}, \\
\theta &= \frac{\Delta - S^2}{S}, \\
a_0 &= \frac{-S\Gamma}{\Delta - S^2}, \\
a_1 &= \frac{\Gamma}{\Delta - S^2}, \\
b &= 1 - \frac{\Gamma^2}{S(\Delta - S^2)}.
\end{aligned}
$$

Therefore, the gamma mixture of normals is fully specified by α, σ_0 and t_{ex} in the SABR.

2.3 Numerical Experiments and Empirical Calibration of SABR

All pricing methods require the SABR model parameters as inputs, which are set for empirical studies in what follows. Now let us introduce the data we use.

For different underlying asset types, there are different channels to obtain related option contracts information. Trading information for equity can be found on YAHOO! Finance channel. As for other underlying asset types such as energy, foreign exchange, interest rates and weather, option contracts in trading are often listed on CME Group website. In our study, we will use Microsoft stock, MSFT, as an example for equity, and iShare 20+ years treasury bond ETF, TLT, as an example of fixed income product. We will price the European options on these assets as of March 28th 2016 that will expire on May 20th 2016.

Figures 13 and 14 show option chains of MSFT and TLT on March 28th 2016 that expire on May 20th 2016. An option chain is simply a sequence of call and put

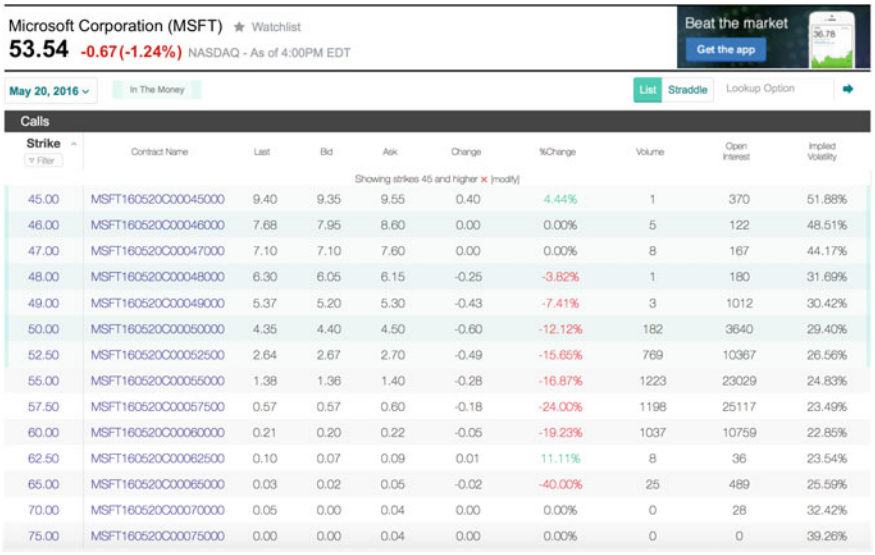

Microsoft Corporation (MSFT) ★ Watchlist
53.54 -0.67(-1.24%) NASDAQ - As of 4:00PM EDT

Beat the market
Get the app

May 20, 2016 | In The Money | List | Straddle | Lookup Option

Calls

Showing strikes 45 and higher | modify

Strike	Contract Name	Last	Bid	Ask	Change	%Change	Volume	Open Interest	Implied Volatility
45.00	MSFT160520C00045000	9.40	9.35	9.55	0.40	4.44%	1	370	51.88%
46.00	MSFT160520C00046000	7.68	7.95	8.60	0.00	0.00%	5	122	48.51%
47.00	MSFT160520C00047000	7.10	7.10	7.60	0.00	0.00%	8	167	44.17%
48.00	MSFT160520C00048000	6.30	6.05	6.15	-0.25	-3.82%	1	180	31.69%
49.00	MSFT160520C00049000	5.37	5.20	5.30	-0.43	-7.41%	3	1012	30.42%
50.00	MSFT160520C00050000	4.35	4.40	4.50	-0.60	-12.12%	182	3640	29.40%
52.50	MSFT160520C00052500	2.64	2.67	2.70	-0.49	-15.65%	769	10367	26.56%
55.00	MSFT160520C00055000	1.38	1.36	1.40	-0.28	-16.87%	1223	23029	24.83%
57.50	MSFT160520C00057500	0.57	0.57	0.60	-0.18	-24.00%	1198	25117	23.49%
60.00	MSFT160520C00060000	0.21	0.20	0.22	-0.05	-19.23%	1037	10759	22.85%
62.50	MSFT160520C00062500	0.10	0.07	0.09	0.01	11.11%	8	36	23.54%
65.00	MSFT160520C00065000	0.03	0.02	0.05	-0.02	-40.00%	25	489	25.59%
70.00	MSFT160520C00070000	0.05	0.00	0.04	0.00	0.00%	0	28	32.42%
75.00	MSFT160520C00075000	0.00	0.00	0.04	0.00	0.00%	0	0	39.26%

Fig. 13 Microsoft stock option chain

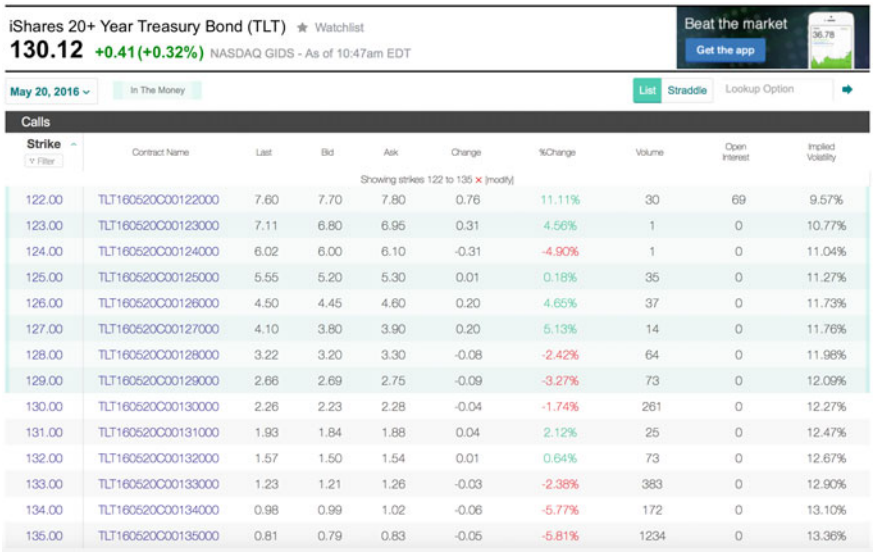

iShares 20+ Year Treasury Bond (TLT) ★ Watchlist
130.12 +0.41(+0.32%) NASDAQ GIDS - As of 10:47am EDT

Beat the market
Get the app

May 20, 2016 | In The Money | List | Straddle | Lookup Option

Calls

Showing strikes 122 to 135 | modify

Strike	Contract Name	Last	Bid	Ask	Change	%Change	Volume	Open Interest	Implied Volatility
122.00	TLT160520C00122000	7.60	7.70	7.80	0.76	11.11%	30	69	9.57%
123.00	TLT160520C00123000	7.11	6.80	6.95	0.31	4.56%	1	0	10.77%
124.00	TLT160520C00124000	6.02	6.00	6.10	-0.31	-4.90%	1	0	11.04%
125.00	TLT160520C00125000	5.55	5.20	5.30	0.01	0.18%	35	0	11.27%
126.00	TLT160520C00126000	4.50	4.45	4.60	0.20	4.65%	37	0	11.73%
127.00	TLT160520C00127000	4.10	3.80	3.90	0.20	5.13%	14	0	11.76%
128.00	TLT160520C00128000	3.22	3.20	3.30	-0.08	-2.42%	64	0	11.98%
129.00	TLT160520C00129000	2.66	2.69	2.75	-0.09	-3.27%	73	0	12.09%
130.00	TLT160520C00130000	2.26	2.23	2.28	-0.04	-1.74%	261	0	12.27%
131.00	TLT160520C00131000	1.93	1.84	1.88	0.04	2.12%	25	0	12.47%
132.00	TLT160520C00132000	1.57	1.50	1.54	0.01	0.64%	73	0	12.67%
133.00	TLT160520C00133000	1.23	1.21	1.26	-0.03	-2.38%	383	0	12.90%
134.00	TLT160520C00134000	0.98	0.99	1.02	-0.06	-5.77%	172	0	13.10%
135.00	TLT160520C00135000	0.81	0.79	0.83	-0.05	-5.81%	1234	0	13.36%

Fig. 14 iShare 20+ year treasury bond option chain

option strike prices along with their premiums for a given maturity period (cf. Harris 2003).

To fully describe the SABR model, we need an initial volatility and a risk-free interest rate. We use the historical volatility up to the as-of-date as a proxy of volatility

NOTE: futures symbols begin with the character @
index symbols begin with the character $

Symbol (option symbols)	hv20	hv50	hv100	DATE	curiv	Days/Percentile	Close
**********							
* Data generated by McMillan Analysis Corp. Copyright 2016 *							
* www.optionstrategist.com 800-724-1817 *							
**********							
$AUM	15	13	12	160324	12.86	597/ 97%ile	75.28
$AUX	15	13	12	160324	17.03	600/ 47%ile	132.86
$BKX	26	33	28	160208	34.55	426/ 99%ile	64.80
$BPX	11	12	10	160324	15.86	599/ 99%ile	70.66
$BRB	26	22	20	160119	29.09	346/ 71%ile	368.08
$BVZ	89	107	131	160324	45.21	251/ 55%ile	14.74
$CDD	13	13	11	160324	12.79	600/ 83%ile	132.49
$DJX	10	18	17	160324	12.89	600/ 66%ile	175.16
$EPX	89	87	72	150821	47.10	441/ 97%ile	192.89
$EUI	10	9	10	160324	10.80	597/ 50%ile	89.49
$EUU	9	9	10	160324	12.23	600/ 65%ile	111.74
$GBP	11	11	10	160324	12.94	598/ 98%ile	141.54
$GVZ	67	109	96	150402	136.07	573/ 95%ile	14.60
$HGX	16	26	25	160324	22.68	598/ 50%ile	224.78
$MNX	15	24	21	160324	19.26	585/ 80%ile	440.55
$NDO	17	15	13	160324	12.80	597/ 87%ile	67.01
$NDX	15	24	21	160324	13.06	595/ 49%ile	4405.53
$NZD	17	15	13	160324	16.05	600/ 24%ile	149.25
$OEX	12	19	18	160324	12.55	591/ 63%ile	904.06
$OSX	44	49	43	160324	36.06	480/ 90%ile	157.82
$OVX	58	70	72	150512	101.87	581/ 90%ile	33.70
$PZO	14	16	13	160324	19.67	600/ 72%ile	176.11
$RUI	13	19	18	151020	9.62	468/ 0%ile	1124.50
$RUT	20	24	21	160324	16.06	598/ 66%ile	1079.54
$RVX	84	87	96	160324	164.29	570/ 94%ile	19.40
$SFC	8	9	10	160324	10.10	597/ 37%ile	97.57
$SKA	9	8	9	160324	12.55	597/ 31%ile	82.95
$SOX	17	29	25	160324	27.23	569/ 74%ile	666.14
$SPX	12	19	18	160324	12.74	600/ 67%ile	2035.94
$VIX	89	107	131	160324	80.08	600/ 40%ile	14.74
$VXEEM	63	84	93	150331	77.40	486/ 23%ile	18.16
$VXEWZ	60	65	64	150406	70.48	494/ 38%ile	33.85
$VXST	132	157	193	150609	139.86	287/ 24%ile	15.22
$XAU	55	55	54	160324	49.05	598/ 86%ile	67.48

Fig. 15 Historical volatilities

initialization. This piece of information is provided by Option Strategist website to each traded underlying asset.

In Fig. 15, each underlying asset has three historical at-the-money volatilities based on the window length used to calculate that volatility. For example, there are three historical volatilities associated with MSFT, 24, 31 and 26%, which are calculated from 20, 50 and 100 days historical volatility respectively as of March 24th 2016. And the volatility of MSFT on that day is 20.82%.

Risk-free interest rate is the minimum rate of return an investor should expect for any investment. In practice, three-month U.S. Treasury bill is often used as a proxy of

Date	1 Mo	3 Mo	6 Mo	1 Yr	2 Yr	3 Yr	5 Yr	7 Yr	10 Yr	20 Yr	30 Yr
03/01/16	0.29	0.33	0.50	0.68	0.85	0.98	1.31	1.62	1.83	2.28	2.70
03/02/16	0.28	0.36	0.48	0.67	0.85	1.00	1.34	1.65	1.84	2.27	2.69
03/03/16	0.25	0.28	0.46	0.65	0.85	0.99	1.33	1.63	1.83	2.23	2.65
03/04/16	0.25	0.29	0.47	0.67	0.88	1.04	1.38	1.69	1.88	2.29	2.70
03/07/16	0.27	0.32	0.49	0.67	0.91	1.08	1.42	1.72	1.91	2.30	2.71
03/08/16	0.27	0.29	0.48	0.68	0.88	1.04	1.34	1.64	1.83	2.22	2.63
03/09/16	0.27	0.30	0.47	0.68	0.90	1.07	1.39	1.69	1.90	2.27	2.68
03/10/16	0.27	0.32	0.50	0.69	0.93	1.11	1.45	1.75	1.93	2.29	2.70
03/11/16	0.27	0.33	0.51	0.70	0.97	1.16	1.49	1.79	1.98	2.34	2.75
03/14/16	0.28	0.34	0.52	0.70	0.97	1.15	1.49	1.78	1.97	2.33	2.74
03/15/16	0.29	0.34	0.52	0.71	0.98	1.16	1.50	1.78	1.97	2.33	2.73
03/16/16	0.28	0.31	0.47	0.66	0.87	1.05	1.41	1.72	1.94	2.32	2.73
03/17/16	0.29	0.29	0.47	0.64	0.87	1.04	1.39	1.70	1.91	2.28	2.69
03/18/16	0.27	0.30	0.44	0.62	0.84	1.00	1.34	1.66	1.88	2.26	2.68
03/21/16	0.26	0.31	0.46	0.63	0.87	1.05	1.38	1.70	1.92	2.31	2.72
03/22/16	0.28	0.30	0.46	0.64	0.91	1.08	1.42	1.74	1.94	2.32	2.72
03/23/16	0.27	0.30	0.46	0.64	0.87	1.03	1.37	1.67	1.88	2.25	2.65
03/24/16	0.24	0.30	0.46	0.63	0.89	1.05	1.39	1.70	1.91	2.28	2.67
03/28/16	0.19	0.29	0.49	0.65	0.89	1.04	1.37	1.68	1.89	2.26	2.66
03/29/16	0.18	0.23	0.45	0.63	0.78	0.94	1.29	1.59	1.81	2.20	2.60
03/30/16	0.14	0.20	0.39	0.61	0.76	0.91	1.26	1.60	1.83	2.24	2.65

Fig. 16 Daily treasury yield curve rates

risk-free interest rate. U.S. Department of the Treasury releases daily treasury yield curves on its website, where we quote our risk-free interest rate. See Fig. 16.

Fitting SABR model parameters is not always straight forward because some of them are not observable from market. Therefore, we determine reasonable ranges for each of α and ρ, and simulate European call option prices in scenarios with different price-volatility correlation ρ and vol of vol α combinations.

Tables 3 and 4 specify SABR model parameters for MSFT and TLT respectively.

Table 5 shows MSFT option prices computed by the brute-force Monte-Carlo (Monte-Carlo column), and by dimension reduction methods we proposed using different distributions for (Σ^2, X_2), i.e. gamma mixture of normals (Gamma column), inverse-gamma mixture of normals (Inverse Gamma column) and log-normal mixture of normals (Log Normal column) respectively. As an option price is not known a priori at the time of pricing, we assume the brute-force MC gives a benchmark price. As for computational efficiency, the proposed approximation methods with different distributions all turn out to be much faster than the brute-force MC, and the results they produced also fall into a satisfactory range of accuracy. Figures 17 and 18 demonstrate pricing errors (see the caption of Fig. 17 for the definition) by using gamma mixture of normals. Note that the quality of the proposed approximation scheme depends on the parameter values. It is observed that the pricing is less accurate when ρ is near -1 than when ρ is near zero due to the leverage effect. And

Table 3 Model parameters microsoft stock

Item	Symbol	Value
Strike price	K	\$52.50
Closing price	F_0	\$53.54
Initial volatility	σ_0	26.56%
Time to maturity	t_{ex}	39
Risk-free interest rate	r	0.29%
Correlation	ρ	$[-1, 0]$
Vol of Vol	α	$[0, 1]$

Table 4 Model Parameters iShare 20+ years Treasury Bond ETF

Item	Symbol	Value
Strike price	K	\$125.00
Closing price	F_0	\$130.12
Initial volatility	σ_0	11.27%
Time to maturity	t_{ex}	39
Risk-free interest Rate	r	0.29%
Correlation	ρ	$[-1, 0]$
Vol of Vol	α	$[0, 1]$

Table 5 $\beta = 1$ SABR model prices comparison

α	ρ	Monte-Carlo	Gamma	Inverse gamma	Log normal
0.10	−0.05	2.86	2.86	2.85	2.86
0.10	−0.15	2.85	2.89	2.85	2.90
0.10	−0.25	2.83	2.90	2.92	2.86
0.10	−0.35	2.86	2.84	2.90	2.84
0.10	−0.45	2.84	2.92	2.89	2.89
0.10	−0.55	2.83	2.80	2.84	2.91
0.10	−0.65	2.84	2.79	2.87	2.99
0.10	−0.75	2.83	2.86	2.69	2.74
0.10	−0.85	2.85	2.77	2.83	2.69
0.10	−0.95	2.88	2.90	3.00	2.72
0.20	−0.05	2.85	2.86	2.86	2.86
0.20	−0.15	2.88	2.87	2.86	2.86
0.20	−0.25	2.85	2.89	2.92	2.97

(continued)

Table 5 (continued)

α	ρ	Monte-Carlo	Gamma	Inverse gamma	Log normal
0.20	−0.35	2.88	2.88	2.87	2.92
0.20	−0.45	2.87	2.94	2.90	2.83
0.20	−0.55	2.86	2.92	2.87	2.88
0.20	−0.65	2.86	2.82	2.92	2.83
0.20	−0.75	2.85	2.78	2.83	2.93
0.20	−0.85	2.86	2.87	2.92	2.79
0.20	−0.95	2.87	3.37	3.22	2.99
0.30	−0.05	2.84	2.87	2.87	2.87
0.30	−0.15	2.85	2.89	2.89	2.86
0.30	−0.25	2.87	2.89	2.92	2.83
0.30	−0.35	2.86	2.98	2.90	2.96
0.30	−0.45	2.86	2.90	2.93	2.87
0.30	−0.55	2.88	2.93	2.81	2.80
0.30	−0.65	2.87	2.93	2.83	2.93
0.30	−0.75	2.86	2.87	2.89	2.69
0.30	−0.85	2.86	2.63	2.87	2.95
0.30	−0.95	2.88	2.71	2.81	3.01
0.40	−0.05	2.86	2.87	2.87	2.87
0.40	−0.15	2.85	2.87	2.88	2.89
0.40	−0.25	2.86	2.87	2.91	2.89
0.40	−0.35	2.86	2.90	2.93	2.88
0.40	−0.45	2.84	2.88	2.88	3.00
0.40	−0.55	2.86	3.00	2.90	2.93
0.40	−0.65	2.86	2.99	3.03	2.89
0.40	−0.75	2.86	2.96	3.03	2.92
0.40	−0.85	2.89	2.77	3.00	3.07
0.40	−0.95	2.90	2.75	2.80	2.71
0.50	−0.05	2.87	2.88	2.86	2.88
0.50	−0.15	2.88	2.89	2.88	2.87
0.50	−0.25	2.86	2.88	2.86	2.89
0.50	−0.35	2.85	2.88	2.86	2.89
0.50	−0.45	2.87	2.89	2.92	2.86
0.50	−0.55	2.87	2.95	2.97	2.84
0.50	−0.65	2.84	2.77	2.84	2.89
0.50	−0.75	2.86	2.92	2.98	2.77
0.50	−0.85	2.91	2.82	2.80	2.96
0.50	−0.95	2.89	2.86	2.69	3.08
0.60	−0.05	2.87	2.86	2.88	2.87

(continued)

Table 5 (continued)

α	ρ	Monte-Carlo	Gamma	Inverse gamma	Log normal
0.60	−0.15	2.85	2.89	2.89	2.90
0.60	−0.25	2.87	2.90	2.90	2.92
0.60	−0.35	2.88	2.95	2.92	2.90
0.60	−0.45	2.88	2.81	2.95	3.00
0.60	−0.55	2.89	2.89	2.99	2.86
0.60	−0.65	2.87	2.92	2.88	2.88
0.60	−0.75	2.87	2.92	2.76	3.13
0.60	−0.85	2.89	2.80	2.83	2.80
0.60	−0.95	2.88	3.02	3.09	2.90
0.70	−0.05	2.86	2.86	2.88	2.89
0.70	−0.15	2.86	2.90	2.90	2.89
0.70	−0.25	2.89	2.92	2.93	2.90
0.70	−0.35	2.87	2.92	2.93	2.93
0.70	−0.45	2.88	3.03	2.89	2.95
0.70	−0.55	2.89	2.94	2.88	2.91
0.70	−0.65	2.88	2.82	2.91	2.91
0.70	−0.75	2.90	2.99	2.73	2.90
0.70	−0.85	2.87	2.93	2.91	2.97
0.70	−0.95	2.88	2.89	2.82	2.97
0.80	−0.05	2.89	2.91	2.87	2.91
0.80	−0.15	2.89	2.90	2.90	2.90
0.80	−0.25	2.90	2.94	2.88	2.91
0.80	−0.35	2.86	2.91	2.91	2.93
0.80	−0.45	2.88	2.94	2.86	2.87
0.80	−0.55	2.89	2.91	2.93	2.83
0.80	−0.65	2.88	2.97	2.95	2.89
0.80	−0.75	2.90	2.92	2.80	2.87
0.80	−0.85	2.89	3.03	2.98	2.87
0.80	−0.95	2.89	2.78	2.71	2.60
0.90	−0.05	2.88	2.87	2.90	2.87
0.90	−0.15	2.90	2.91	2.91	2.91
0.90	−0.25	2.89	2.93	2.93	2.92
0.90	−0.35	2.90	2.94	2.90	2.90
0.90	−0.45	2.91	2.98	2.98	2.94
0.90	−0.55	2.90	2.96	2.91	2.94
0.90	−0.65	2.89	3.11	2.97	3.00
0.90	−0.75	2.89	2.87	2.84	2.84
0.90	−0.85	2.90	2.83	2.75	2.89

(continued)

Table 5 (continued)

α	ρ	Monte-Carlo	Gamma	Inverse gamma	Log normal
0.90	−0.95	2.88	2.81	2.82	2.78
1.00	−0.05	2.89	2.90	2.87	2.88
1.00	−0.15	2.87	2.91	2.92	2.91
1.00	−0.25	2.86	2.94	2.92	2.92
1.00	−0.35	2.89	2.98	2.91	2.93
1.00	−0.45	2.90	3.02	2.90	2.93
1.00	−0.55	2.91	2.95	2.86	2.87
1.00	−0.65	2.90	2.88	2.85	2.92
1.00	−0.75	2.90	2.86	2.80	2.95
1.00	−0.85	2.91	2.91	2.83	2.87
1.00	−0.95	2.89	2.96	2.81	3.04

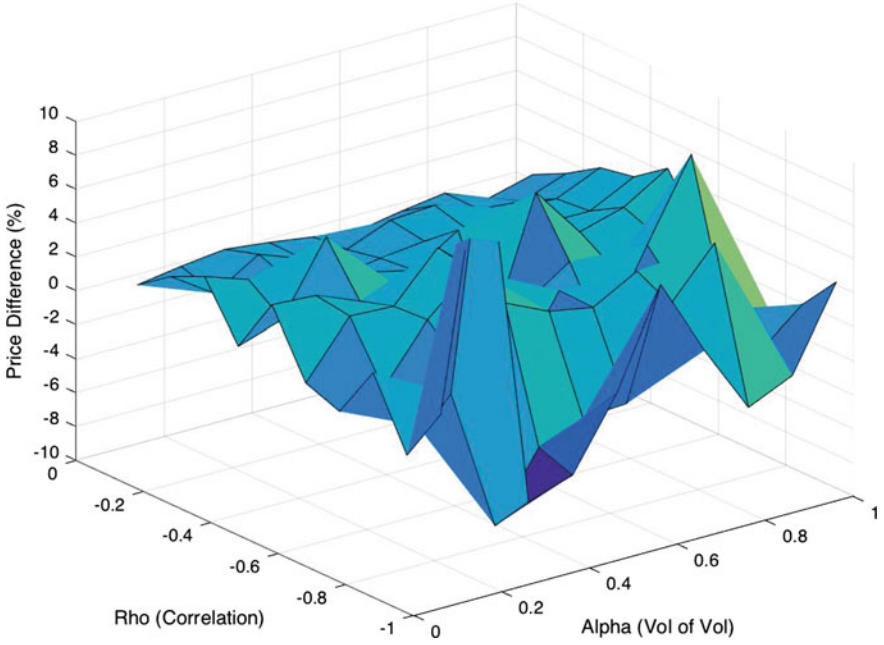

Fig. 17 Pricing error for the case $\beta = 1$, dimension reduction MC using gamma mixture of normal versus brute-force MC: let P_{DR} = option price computed using the dimension reduction MC, and P_{BF} = option price computed using the brute-force MC, then (y-coordinate)/100 = $\frac{P_{DR}-P_{BF}}{P_{BF}}$

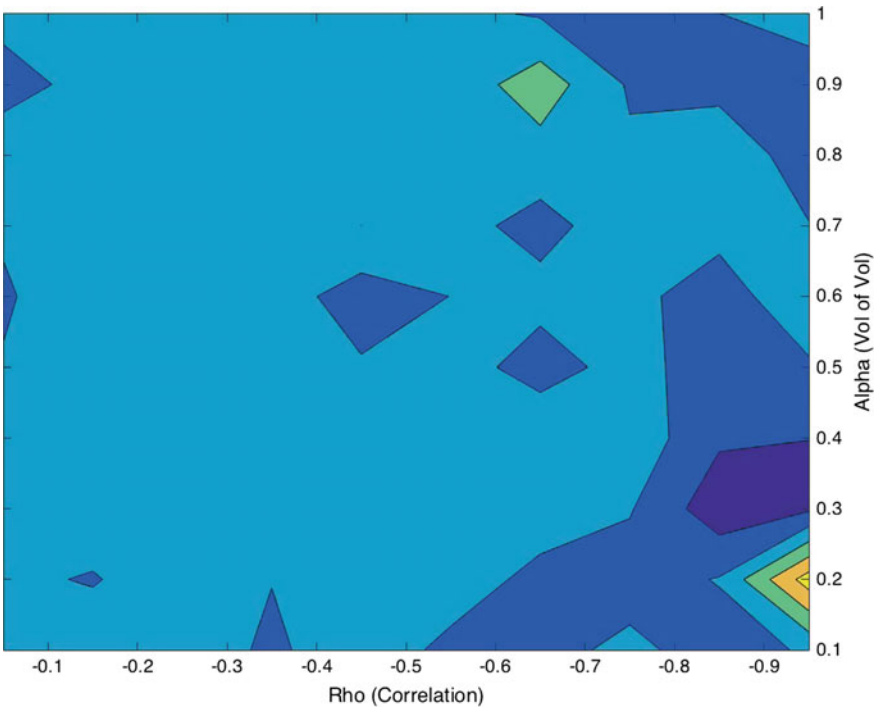

Fig. 18 *Top* view of Fig. 17: the large *light blue* area contains pairs (α, ρ) that yield small pricing errors compared to areas of other colors

greater values of α (volatility of volatility) tends to yield a better result, perhaps due to a greater degree of "mixing" in Monte-Carlo simulation. Table 5 covers a wide spectrum of combinations between α and ρ. Moreover, results using the other two approximate distributions, although not presented in this chapter, are in fact more stable. See Yin (2016) for detailed accounts.

References

Antonov, A., & Spector, M. (2012). Advanced analytics for the SABR model. *SSRN 2026350*.

Brooks, S., Gelman, A., Jones, G., & Meng, X.L. (2011). *Handbook of markov chain Monte-Carlo*. CRC Press.

Das, S. (2005). A learning market maker in the Glosten-Milgrom model. *Quantitative Finance*, *5*(2), 169–180.

Dempster, A. P., Laird, N. M., & Rubin, D. B. (1977). Maximum likelihood from incomplete data via EM algorithm (with discussion). *Journal of Royal Statistical Society, Series B*, *39*, 1–38.

Gelman, A., & Rubin, D. (1992). Inference from iterative simulation using multiple sequences. *Statistical Science*, *7*(4), 457–472.

Geweke, J. (1992). Evaluating the accuracy of sampling-based approaches to the calculation of posterior moments. *Bayesian Statistics*, 169–193.

Glosten, L., & Milgrom, P. (1985). Bid, ask and transaction prices in a specialist market with heterogeneously informed traders. *Journal of Financial Economics*, *14*(1), 71–100.

Hagan, P., Kumar, D., Lesniewski, A., & Woodward, D. (2002). Managing smile risk. *The Best of Wilmott*, 249–296.

Hagan, P., Lesniewski, A., & Woodward, D. (2005). Probability distribution in the SABR model of stochastic volatility. *Large deviations and asymptotic methods in finance* (pp. 1–35). Springer.

Harris, L. (2003). *Trading and exchanges*. Oxford University Press.

Hasbrouck, J. (2009). Trading costs and returns for US equities: estimating effective costs from daily data. *Journal of Finance*, *64*(3), 1–52.

Meng, X. L., & van Dyk, D. (1997). The EM algorithm: an old folk-song sung to a fast new tune (with discussion). *Journal of Royal Statistical Society, Series B*, *59*, 511–568.

Paulot, L. (2009). Asymptotic implied volatility at the second order with application to the SABR model. *SSRN 1413649*.

Rebonado, R., McKay, K., & White, R. (2011). *The SABR/LIBOR market model: Pricing, calibration and hedging for complex interest-rate derivatives*. Wiley.

Robert, C., & Casella, G. (2004). *Monte-Carlo statistical methods* (2nd ed.). Springer.

Roll, R. (1984). A simple implicit measure of the effective bid-ask spread in an efficient market. *Journal of Finance*, *39*(4), 1127–1139.

Wang, T. (2014). *Empirical analysis of sequential trade models for market microstructure*. Ph.D. thesis, University of North Carolina at Chapel Hill.

Yin, L. (2016). *Monte-Carlo strategies in option pricing for SABR model*. Ph.D. thesis, University of North Carolina at Chapel Hill.